J. Phys. A: Math. Gen. **32** (1999) 4897–4906. Printed in the UK PII: S0305-4470(99)01723-0

Coupling-anisotropy and finite-size effects in interfacial tension of the two-dimensional Ising model

Ming-Chya Wu†, Ming-Chang Huang†§, Yu-Pin Luo† and Tsong-Ming Liaw†‡

† Department of Physics, Chung-Yuan Christian University, Chungli 320, Taiwan, Republic of China
‡ Computing Centre, Academia Sinica, Nankang 115, Taiwan, Republic of China
§ Department of Physics, Chung-Yuan Christian University, Chungli 320, Taiwan, Republic of China

E-mail: `ming@phys.cycu.edu.tw` (Ming-Chang Huang)

Received 8 February 1999, in final form 8 April 1999

Abstract. Exact expressions of the Bloch wall free energy are obtained for the Ising model on a rectangular lattice and infinitely long cylinder. The interfacial tension amplitudes are obtained for different coupling and aspect ratios. Finite-size scaling theory is used to analyse the effects of coupling anisotropy and finite size in the interfacial tension.

The interfacial free energies are defined as the difference between the free energies of two finite-size systems with different boundary conditions. For the case of an Ising model, the difference in free energy between a system with periodic and antiperiodic boundary conditions is sometimes referred to as the Bloch wall free energy [1], which is the case we analyse in this work. Consider an Ising model defined on a $L_x \times L_y$ rectangular lattice with periodic boundary condition along L_x. The boundary condition along L_y is periodic or antiperiodic. Then the interfacial tension, which is the interfacial free energy per unit length and per $k_B T$, is

$$\sigma\left(t, \frac{J_2}{J_1}; L_x, L_y\right) = L_y\left[f_{pa}\left(t, \frac{J_2}{J_1}; L_x, L_y\right) - f_{pp}\left(t, \frac{J_2}{J_1}; L_x, L_y\right)\right] \quad (1)$$

where J_1 and J_2 are the couplings along L_x and L_y respectively, t is the reduced temperature, $t = (\theta_c - \theta)/\theta_c$ with $\theta = k_B T/J_1$ and $\theta_c = k_B T_c/J_1$, f_{pa} is the free energy density per $k_B T$ for the antiperiodic boundary condition along L_y, and f_{pp} is for the periodic boundary condition along L_y. Note that we choose the coupling along the x-axis, J_1, as the scale to measure the temperature. From the usual scaling ansatz, we can write the scaling form of σ as [2, 3]

$$\sigma(t, r_1; L_x, L_y) = L_x^{-1}\Sigma(tL_x^{1/\nu}; r_1, r_2) \quad (2)$$

where $\Sigma(z; r_1, r_2)$ with $z = tL_x^{1/\nu}$ is the scaling function, r_1 defined as J_2/J_1 is the coupling ratio, and r_2 defined as L_y/L_x is the aspect ratio, and we use the form,

$$\Sigma(z; r_1, r_2) = a_{L_x}(r_1, r_2) + b(r_1, r_2)z \quad (3)$$

0305-4470/99/264897+10$30.00

to approximate the scaling function. We define $A(r_1, r_2)$ as the value of $a_{L_x}(r_1, r_2)$ in the limit of large lattice size,

$$A(r_1, r_2) \equiv \lim_{L_x \gg \xi} a_{L_x}(r_1, r_2) \tag{4}$$

where ξ is the fluctuation length of the interfacial energy for given values of r_1 and r_2, and the value of $A(r_1, r_2)$ is the amplitude of σ at the critical point. For the isotropic coupling, it was known [4] that

$$A(1, 1) = \ln(1 + 2^{3/4}) \approx 0.9865 \tag{5}$$

and the various values of $A(1, r_2)$ for different r_2. In this work, the finite-size dependence of $a_{L_x}(r_1, r_2)$ is proposed to be of the form

$$a_{L_x}(r_1, r_2) = A(r_1, r_2)[1 + a_1(r_1, r_2)x + a_2(r_1, r_2)x^2 + \cdots] \tag{6}$$

with $x = 1/L_x^2$. This proposed form comes from our data analysis, and it reflects the fact that the finite-size correction is very small. For the case of an infinitely long Ising cylinder, i.e. $L_x \to \infty$, the scaling form of σ can be written as

$$\sigma(t, r_1; L_x \to \infty, L_y) = L_y^{-1}\tilde{\Sigma}(tL_y^{1/\nu}; r_1, r_2 = 0) = L_y^{-1}\tilde{\Sigma}(tL_y^{1/\nu}; r_1). \tag{7}$$

Similar to equation (3), we use the form of

$$\tilde{\Sigma}(z; r_1) = \tilde{a}_{L_y}(r_1) + \tilde{b}(r_1)z \tag{8}$$

with $z = tL_y^{1/\nu}$, to approximate the scaling function. Also similar to the case of finite L_x, we define $\tilde{A}(r_1)$ as the value of $\tilde{a}_{L_y}(r_1)$ in the limit of large lattice size,

$$\tilde{A}(r_1) \equiv \lim_{L_y \gg \xi} \tilde{a}_{L_y}(r_1) \tag{9}$$

and the finite-size dependence of $\tilde{a}_{L_y}(r_1)$ is proposed to be

$$\tilde{a}_{L_y}(r_1) = \tilde{A}(r_1)[1 + \tilde{a}_1(r_1)y + \tilde{a}_2(r_1)y^2 + \cdots] \tag{10}$$

with $y = 1/L_y^2$. The value of $\tilde{A}(1)$ is known to be $\pi/4$ [1, 4]. Note that the scale of finite size used in the scaling function of equations (2) and (7) is different, and we have

$$\lim_{\substack{r_2 \to 0 \\ L_y \text{ fixed}}} r_2 \cdot \Sigma(tL_x^{1/\nu}, r_1; r_2) = \tilde{\Sigma}(tL_y^{1/\nu}; r_1). \tag{11}$$

In this paper we report our study on the effects caused by the coupling anisotropy of the couplings and the finite size in the scaling functions of equations (3) and (8), based on the analytic solutions of the two-dimensional Ising model on rectangular lattices and an infinitely long cylinder.

The Hamiltonian of the model defined on a rectangular lattice is written as

$$H = -\sum_{m=1}^{L_x}\sum_{n=1}^{L_y}(J_1\sigma_{m,n}\sigma_{m+1,n} + J_2\sigma_{m,n}\sigma_{m,n+1}) \tag{12}$$

and, up to a factor, the partition function takes the form of

$$Q(L_x, L_y) = \sum_{\{\sigma\}}\left\{\prod_{m=1}^{L_x}\prod_{n=1}^{L_y}(1 + t_1\sigma_{m,n}\sigma_{m+1,n})(1 + t_2\sigma_{m,n}\sigma_{m,n+1})\right\} \tag{13}$$

where $t_1 = \tanh(J_1/k_BT)$ and $t_2 = \tanh(J_2/k_BT)$. The analytic solution of equation (13) for the case of no external field was first solved by Onsager in the limit of an infinitely large lattice [4]. Since then the method of obtaining the analytic solution has been perfected

and reformulated, and the solution for the case of a finite lattice has also been obtained [5–8]. Among these developments, Plechko used a nonstandard and simple approach [9–11], which is based on the Grassmann path-integral factorization of the Boltzmann weights and the principle of mirror ordering of the arising Grassmann factors, to obtain an analytic expression of the partition function of the model on a torus [9]. Based on Plechko's approach, we are able to extend the solution to different cases, including the model on a torus but with an antiperiodic boundary condition and on an infinite cylinder with a periodic or antiperiodic boundary condition. In the following we give a brief review of this method. First, one associates two pairs of conjugate Grassmann variables, $\{a_{m,n}, a^*_{m,n}; b_{m,n}, b^*_{m,n}\}$, to a lattice site (m, n), and we rewrite the Boltzmann weights as

$$1 + t_1\sigma_{m,n}\sigma_{m+1,n} = \int \mathrm{d}a^*_{m,n} \int \mathrm{d}a_{m,n}\, \mathrm{e}^{a_{m,n}a^*_{m,n}}(1 + a_{m,n}\sigma_{m,n})(1 + t_1 a^*_{m,n}\sigma_{m+1,n}) \tag{14}$$

and

$$1 + t_2\sigma_{m,n}\sigma_{m,n+1} = \int \mathrm{d}b^*_{m,n} \int \mathrm{d}b_{m,n}\, \mathrm{e}^{b_{m,n}b^*_{m,n}}(1 + b_{m,n}\sigma_{m,n})(1 + t_2 b^*_{m,n}\sigma_{m,n+1}). \tag{15}$$

The periodic boundary condition along L_x and L_y is equivalent to the condition $\{a^*_{0,n} = -a^*_{L_x,n}, b^*_{m,0} = -b^*_{m,L_y}\}$ for the Grassmann variables. Then one applies the principle of mirror ordering to the Grassmann factors to group together the factors containing the same Ising spin $\sigma_{m,n}$ so that the sum over spin variables can be carried out. After performing the sum over spin variables, one obtains a purely Grassmann representation for the partition function which is

$$Q_{pp}(L_x, L_y) = \tfrac{1}{2}[G|_{\Gamma_1} + G|_{\Gamma_2} + G|_{\Gamma_3} - G|_{\Gamma_4}] \tag{16}$$

where the subscript of Q_{pp} denotes the periodic boundary conditions in both L_x and L_y, G takes the form of

$$G = \int \prod_{m=1}^{L_x}\prod_{n=1}^{L_y}(-\mathrm{d}b^*_{m,n})\,\mathrm{d}a^*_{m,n}\,\mathrm{d}b_{m,n}\,\mathrm{d}a_{m,n}\ \exp\left\{\sum_{m=1}^{L_x}\sum_{n=1}^{L_y}[t_1t_2a^*_{m-1,n}b^*_{m,n-1} + a_{m,n}a^*_{m,n} + b_{m,n}b^*_{m,n} + a_{m,n}b_{m,n} + (t_1a^*_{m-1,n} + t_2b^*_{m,n-1})(a_{m,n} + b_{m,n})]\right\} \tag{17}$$

and the boundary conditions Γ_1, Γ_2, Γ_3, Γ_4 are defined as

$$\Gamma_1 = (a^*_{0,n} = -a^*_{L_x,n}, b^*_{m,0} = -b^*_{m,L_y}) \tag{18}$$

$$\Gamma_2 = (a^*_{0,n} = -a^*_{L_x,n}, b^*_{m,0} = +b^*_{m,L_y}) \tag{19}$$

$$\Gamma_3 = (a^*_{0,n} = +a^*_{L_x,n}, b^*_{m,0} = -b^*_{m,L_y}) \tag{20}$$

$$\Gamma_4 = (a^*_{0,n} = +a^*_{L_x,n}, b^*_{m,0} = +b^*_{m,L_y}). \tag{21}$$

Finally one performs the integration over Grassmann variables by Fourier transform to obtain the result as

$$Q_{pp}(L_x, L_y) = \frac{1}{2}\left[\alpha_1 + \alpha_2 + \alpha_3 - \mathrm{sgn}\left(\frac{\theta - \theta_c}{\theta_c}\right)\alpha_4\right] \tag{22}$$

where

$$\alpha_1 = \prod_{p=0}^{L_x-1}\prod_{q=0}^{L_y-1}\left[\lambda_0 - \lambda_1\cos\frac{2\pi p + \pi}{L_x} - \lambda_2\cos\frac{2\pi q + \pi}{L_y}\right]^{1/2} \tag{23}$$

$$\alpha_2 = \prod_{p=0}^{L_x-1}\prod_{q=0}^{L_y-1}\left[\lambda_0 - \lambda_1\cos\frac{2\pi p + \pi}{L_x} - \lambda_2\cos\frac{2\pi q}{L_y}\right]^{1/2} \tag{24}$$

$$\alpha_3 = \prod_{p=0}^{L_x-1}\prod_{q=0}^{L_y-1}\left[\lambda_0 - \lambda_1\cos\frac{2\pi p}{L_x} - \lambda_2\cos\frac{2\pi q+\pi}{L_y}\right]^{1/2} \tag{25}$$

$$\alpha_4 = \prod_{p=0}^{L_x-1}\prod_{q=0}^{L_y-1}\left[\lambda_0 - \lambda_1\cos\frac{2\pi p}{L_x} - \lambda_2\cos\frac{2\pi q}{L_y}\right]^{1/2} \tag{26}$$

$\lambda_0 = (1+t_1^2)(1+t_2^2)$, $\lambda_1 = 2t_1(1-t_2^2)$, and $\lambda_2 = 2t_2(1-t_1^2)$. Note that the sign factor in front of the last term of equation (22) is equal to +1 for $\theta > \theta_c$ and -1 for $\theta < \theta_c$ with the critical temperature θ_c determined by the equation,

$$\lambda_0 - \lambda_1 - \lambda_2 = 0. \tag{27}$$

We then extend the above method to the cases of different boundary conditions. For the boundary conditions which are periodic along L_x and antiperiodic along L_y, this is equivalent to the condition $\{a^*_{0,n} = -a^*_{L_x,n}, b^*_{m,0} = b^*_{m,L_y}\}$ for the Grassmann variables which amounts to changing the boundary conditions of equation (16) to

$$\Gamma_1 = (a^*_{0,n} = -a^*_{L_x,n}, b^*_{m,0} = +b^*_{m,L_y}) \tag{28}$$

$$\Gamma_2 = (a^*_{0,n} = -a^*_{L_x,n}, b^*_{m,0} = -b^*_{m,L_y}) \tag{29}$$

$$\Gamma_3 = (a^*_{0,n} = +a^*_{L_x,n}, b^*_{m,0} = +b^*_{m,L_y}) \tag{30}$$

$$\Gamma_4 = (a^*_{0,n} = +a^*_{L_x,n}, b^*_{m,0} = -b^*_{m,L_y}) \tag{31}$$

with the same form of G given by equation (17). After carrying out the integration over Grassmann variables, we obtain the result as

$$Q_{pa}(L_x, L_y) = \frac{1}{2}\left[\alpha_1 + \alpha_2 - \alpha_3 + \mathrm{sgn}\left(\frac{\theta-\theta_c}{\theta_c}\right)\alpha_4\right]. \tag{32}$$

For the antiperiodic boundary conditions at both sides, this is equivalent to the condition $\{a^*_{0,n} = a^*_{L_x,n}, b^*_{m,0} = b^*_{m,L_y}\}$ for the Grassmann variables, and the corresponding boundary conditions in equation (16) are

$$\Gamma_1 = (a^*_{0,n} = +a^*_{L_x,n}, b^*_{m,0} = +b^*_{m,L_y}) \tag{33}$$

$$\Gamma_2 = (a^*_{0,n} = +a^*_{L_x,n}, b^*_{m,0} = -b^*_{m,L_y}) \tag{34}$$

$$\Gamma_3 = (a^*_{0,n} = -a^*_{L_x,n}, b^*_{m,0} = +b^*_{m,L_y}) \tag{35}$$

$$\Gamma_4 = (a^*_{0,n} = -a^*_{L_x,n}, b^*_{m,0} = -b^*_{m,L_y}) \tag{36}$$

with the same G. Carrying out the integration over Grassmann variables yields

$$Q_{aa}(L_x, L_y) = \frac{1}{2}\left[-\alpha_1 + \alpha_2 + \alpha_3 + \mathrm{sgn}\left(\frac{\theta-\theta_c}{\theta_c}\right)\alpha_4\right]. \tag{37}$$

It is also interesting to consider the case of an Ising cylinder with $L_x \to \infty$. In this case, equation (22) reduces to

$$\tilde{Q}_p(L_y) \equiv Q_{pp}(L_x \to \infty, L_y) = \lim_{L_x\to\infty}\alpha_3 \tag{38}$$

and equations (32) and (37) reduce to

$$\tilde{Q}_a(L_y) \equiv Q_{pa}(L_x \to \infty, L_y) = Q_{aa}(L_x \to \infty, L_y) = \lim_{L_x\to\infty}\alpha_4. \tag{39}$$

Substituting equations (22) and (32) into equation (1), we obtain the interfacial tension as

$$\sigma(t, r_1; L_x, L_y) = \frac{1}{L_x}\ln\left[\frac{\alpha_1 + \alpha_2 + \alpha_3 - \mathrm{sgn}\left(\frac{\theta-\theta_c}{\theta_c}\right)\alpha_4}{\alpha_1 + \alpha_2 - \alpha_3 + \mathrm{sgn}\left(\frac{\theta-\theta_c}{\theta_c}\right)\alpha_4}\right]. \tag{40}$$

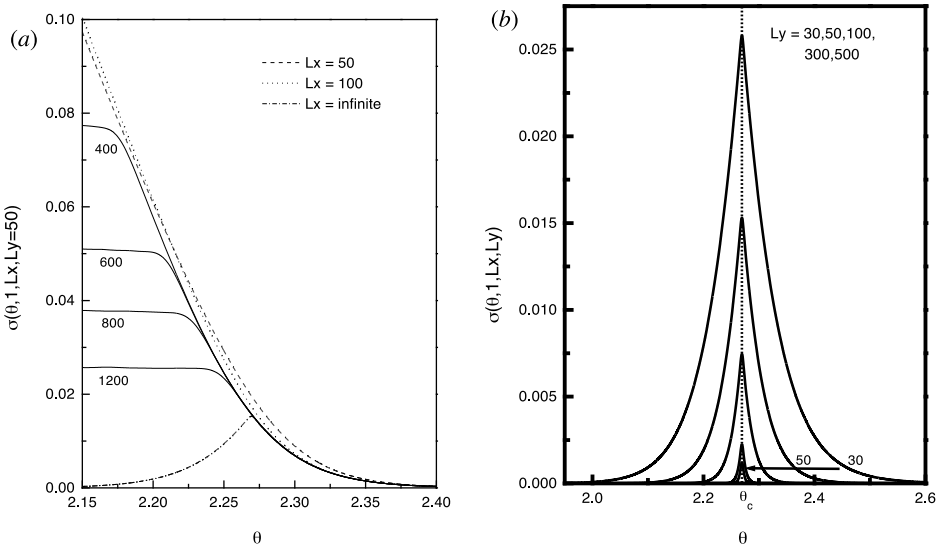

Figure 1. The interfacial tension σ, (*a*) for different L_x and the same $L_y = 50$, and (*b*) for infinitely long cylinders of widths $L_y = 30$, 50, 100, 300, and 500. The coupling ratio is $r_1 = 1$.

For the case of an infinitely long Ising-cylinder, we substitute equations (38) and (39) into equation (1) to obtain the interfacial tension as

$$\sigma(t, r_1; L_x \to \infty, L_y) = \frac{1}{2}\sum_{q=0}^{L_y-1}\int_0^{2\pi}\frac{\mathrm{d}\phi}{2\pi}\ln\left(\frac{\lambda_0 - \lambda_1\cos\phi - \lambda_2\cos\frac{2\pi q+\pi}{L_y}}{\lambda_0 - \lambda_1\cos\phi - \lambda_2\cos\frac{2\pi q}{L_y}}\right) \tag{41}$$

which, after performing the integration, yields

$$\sigma(t, r_1; L_x \to \infty, L_y) = \frac{1}{2}\sum_{q=0}^{L_y-1}\ln\frac{f_1(t, L_y, q) + \sqrt{f_1^2(t, L_y, q) - \lambda_1^2}}{f_2(t, L_y, q) + \sqrt{f_2^2(t, L_y, q) - \lambda_1^2}} \tag{42}$$

with $f_1(t, L_y, q) = \lambda_0 - \lambda_2\cos\frac{2\pi q+\pi}{L_y}$, and $f_2(t, L_y, q) = \lambda_0 - \lambda_2\cos\frac{2\pi q}{L_y}$. In figure 1(*a*), we show the qualitative results of the interfacial tensions σ given by equations (40) and (42) for different values of L_x. For a rectangular lattice, σ is finite in the ordered phase and it vanishes very quickly in the disordered phase when temperature is away from the critical point. But when the aspect ratio r_2 decreases, the global behaviour of σ starts to deviate from this picture, and approaches the result of an infinitely long cylinder. For an infinitely long cylinder, as shown in figure 1(*b*), the peak of σ locates exactly at the critical point, and the value of σ decreases in a symmetrical way from the critical point. This feature persists to the case of anisotropic couplings, and it may provide a very effective way of determining the critical temperature [12–14]. We will illustrate the latter point in a separate paper. In the following, we analyse the surface tension for the ordered phase.

First we consider the interfacial tension at the critical point for the case of isotropic couplings on a rectangular lattice. In this case, using equations (40), (2) and (3) with $\lambda_1 = \lambda_2 = \lambda_0/2$ we obtain the scaling function at the critical point as

$$\Sigma(0; 1, r_2) = a_{L_x}(1, r_2) = \ln\left(\frac{\alpha_1 + \alpha_2 + \alpha_3}{\alpha_1 + \alpha_2 - \alpha_3}\right). \tag{43}$$

Table 1. The values of the parameters in the scaling function, $\Sigma(z; r_1, r_2) = a_{L_x}(r_1, r_2)+b(r_1, r_2)z$, with $a_{L_x}(r_1, r_2) = A(r_1, r_2)[1 + a_1(r_1, r_2)x + \cdots]$ and $x = 1/L_x^2$ for a rectangular lattice with isotropic coupling $r_1 = 1$, and a different aspect ratio, r_2.

r_2	$r_2 \cdot A(1, r_2)$	$a_1(1, r_2)$	$r_2 \cdot b(1, r_2)$
0.1	0.7854(4)	41.049(9)	0.088(0)
0.2	0.7893(0)	10.030(2)	0.179(4)
0.4	0.8357(3)	1.998(5)	0.393(3)
0.5	0.8709(3)	0.991(9)	0.507(9)
1.0	0.9864(9)	−0.298(9)	1.008(2)
1.5	0.9546(3)	−0.513(2)	1.346(3)
2.0	0.8438(2)	−0.665(0)	1.529(3)
2.5	0.7065(0)	−0.818(2)	1.574(8)
3.0	0.5703(9)	−0.974(8)	1.514(7)
3.5	0.4486(0)	−1.133(5)	1.385(3)
4.0	0.3459(3)	−1.293(5)	1.219(0)
4.5	0.2626(9)	−1.454(2)	1.040(7)
5.0	0.1970(5)	−1.615(4)	0.867(2)

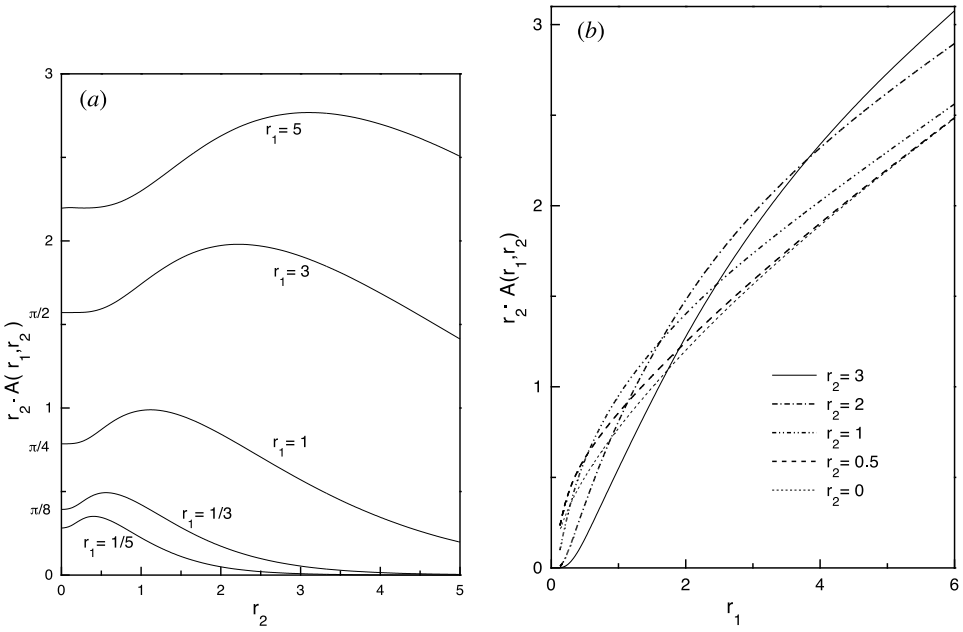

Figure 2. The interfacial tension amplitude multiplied by the aspect ratio r_2 at the critical point (*a*) as a function of r_2 for a given coupling ratio r_1, and (*b*) as a function of coupling ratio r_1 for a given aspect ratio r_2.

For the aspect ratio $r_2 = 1$ and in the limit of large lattice site, equation (43) yields the result of equation (5), $A(1, 1) = 0.986\,4855\ldots$. For other aspect ratios, the results of $r_2 \cdot A(1, r_2)$ are shown in table 1, and the behaviour of $r_2 \cdot A(1, r_2)$ versus r_2 is shown in figure 2(*a*). We then consider the finite-size dependence of the value of $a_{L_x}(1, 1)$ by using the data obtained from equation (43), and we find the best fitting curve is given by the form of equation (6) as $a_{L_x}(1, 1) = A(1, 1)[1 - 0.2989x - 0.3493x^2 + \cdots]$, with $x = 1/L_x^2$ as shown in figure 3. The leading order correction due to the finite-size effect is given by $a_1(1, r_2)$, and the values of

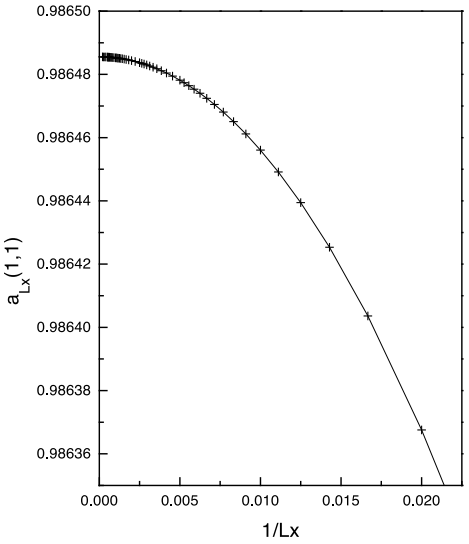

Figure 3. The finite-size dependence to the interfacial tension amplitude at the critical point, $a_{L_x}(r_1, r_2) = A(r_1, r_2)[1 + a_1(r_1, r_2)x + a_2(r_1, r_2)x^2 + \cdots]$, with $x = 1/L_x^2$ for coupling ratio $r_1 = 1$ and aspect ratio $r_2 = 1$. The solid curve is given by $a_{L_x}(1, 1) = 0.986\,4855(1 - 0.2989x - 0.3493x^2)$, and the crossed points are calculated from equation (43).

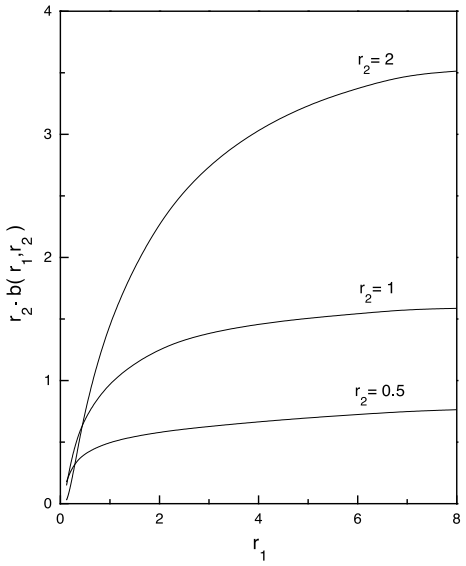

Figure 4. The parameter $b(r_1, r_2)$ in the scaling function, $\Sigma(z; r_1, r_2) = a_{L_x}(r_1, r_2) + b(r_1, r_2)z$ with $z = tL_x^{1/\nu}$, as a function of coupling ratio r_1 for aspect ratio r_2.

$a_1(1, r_2)$ are listed in table 1 for different r_2. Once the values of $a_{L_x}(1, r_2)$ for different size L_x are determined, using equation (40) we can determine the parameter $b(1, r_2)$ of equation (3). The results of $b(1, r_2)$ for different aspect ratios are also shown in table 1, and among them we have $b(1, 1) \approx 1$. For the case of anisotropic couplings on a rectangular lattice where the critical point is determined by equation (27), and the scaling function at the critical point is given by equation (43) with $\lambda_0 = \lambda_1 + \lambda_2$. The results of $A(r_1, 1)$ for different coupling ratios r_1 are listed in table 2, and the behaviour of $r_2 \cdot A(r_1, r_2)$ with respect to r_2 for different r_1 is shown in figure 2(*a*). The behaviour of $r_2 \cdot A(r_1, r_2)$ with respect to r_1 for different r_2 is shown in figure 2(*b*). To see the finite-size correction to $A(r_1, r_2)$ for different r_1, we determine $a_1(r_1, r_2)$, $a_2(r_1, r_2)$ and $b(r_1, r_2)$ of equations (6) and (3), and the results of $a_1(r_1, 1)$ and $b(r_1, 1)$ are listed in table 2. We also show the behaviour of $b(r_1, r_2)$ with respect to r_1 for different r_2 in figure 4.

Then we use equation (42) to consider the interfacial tension for an infinitely long Ising cylinder. For the system with isotropic coupling, $r_1 = 1$, and at the critical point, equation (42) becomes

$$\sigma(0, 1; L_x \to \infty, L_y) = \frac{1}{2}\sum_{q=0}^{L_y-1} \ln \frac{1 - \frac{1}{2}\cos\frac{2\pi q+\pi}{L_y} + \frac{1}{2}\sqrt{3 - 4\cos\frac{2\pi q+\pi}{L_y} + \cos^2\left(\frac{2\pi q+\pi}{L_y}\right)}}{1 - \frac{1}{2}\cos\frac{2\pi q}{L_y} + \frac{1}{2}\sqrt{3 - 4\cos\frac{2\pi q}{L_y} + \cos^2\left(\frac{2\pi q}{L_y}\right)}} \tag{44}$$

which gives $\tilde{A}(1) = \pi/4$. To find the finite-size dependence of the value of $\tilde{a}_{L_y}(1)$, we use the data obtained from equation (44) to find the best fitting curve, which is $\tilde{a}_{L_y}(1) =$

Table 2. The critical temperature θ_c and the values of the parameters in the scaling function, $\Sigma(z; r_1, r_2) = a_{L_x}(r_1, r_2) + b(r_1, r_2)z$, with $a_{L_x}(r_1, r_2) = A(r_1, r_2)[1 + a_1(r_1, r_2)x + \cdots]$ and $x = 1/L_x^2$ for a rectangular lattice with a different coupling ratio r_1, and aspect ratio, $r_2 = 1$.

r_1	θ_c	$A(r_1, 1)$	$a_1(r_1, 1)$	$b(r_1, 1)$
8	7.778 756 01(1)	3.0686(7)	3.136(8)	1.586(6)
7	7.112 386 21(3)	2.8176(2)	2.490(8)	1.577(9)
6	6.423 824 39(7)	2.5614(1)	1.984(8)	1.543(2)
5	5.707 791 57(0)	2.2989(4)	1.506(7)	1.507(6)
4	4.956 311 00(4)	2.0278(3)	1.048(4)	1.459(5)
3	4.156 173 77(9)	1.7418(6)	0.610(0)	1.390(2)
2	3.282 035 81(3)	1.4214(8)	0.177(7)	1.273(4)
1	2.269 185 28(9)	0.9864(9)	−0.298(9)	1.008(2)
$\frac{1}{2}$	1.641 017 91(4)	0.6135(5)	−0.900(5)	0.704(4)
$\frac{1}{3}$	1.385 391 27(7)	0.4219(1)	−1.667(6)	0.522(3)
$\frac{1}{4}$	1.239 077 73(7)	0.3030(9)	−2.700(9)	0.397(5)
$\frac{1}{5}$	1.141 558 30(9)	0.2233(7)	−4.019(1)	0.307(0)
$\frac{1}{6}$	1.070 637 40(9)	0.1674(9)	−5.635(7)	0.239(4)
$\frac{1}{7}$	1.016 055 17(3)	0.1271(9)	−7.542(7)	0.187(9)
$\frac{1}{8}$	0.972 344 52(3)	0.0975(5)	−9.773(0)	0.148(3)

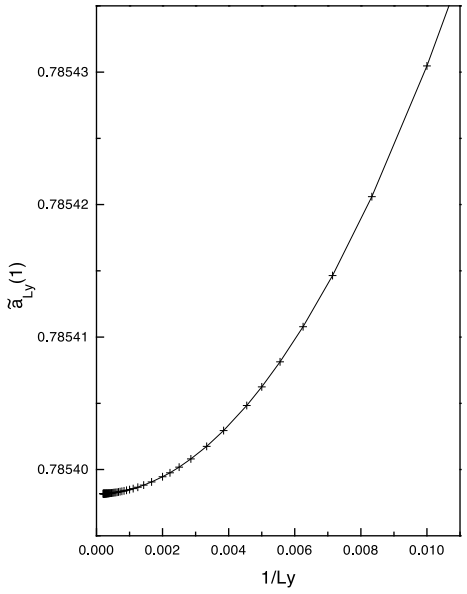

Figure 5. The finite-size dependence of the interfacial tension amplitude at the critical point $\tilde{a}_{L_y}(r_1) = \tilde{A}(r_1)[1 + \tilde{a}_1(r_1)y + \tilde{a}_2(r_1)y^2 + \cdots]$ for coupling ratio $r_1 = 1$. The solid line is given by $\tilde{a}_{L_y}(1) = 0.785\,3982(1 + 0.4113y + 0.6083y^2)$, and the crossed points are calculated from equation (44).

$\tilde{A}(1)[1 + 0.4113y + 0.6083y^2 + \cdots]$. The fitting curve and the data are shown in figure 5. Once $\tilde{a}_{L_y}(r_1)$ are determined, using equation (44) with $\lambda_1 = \lambda_2$ we can determine the parameter $\tilde{b}(1)$ of equation (8), and the result is $\tilde{b}(1) = -0.8790$. Then we extend the calculation to the case $r_1 \neq 1$ to obtain $\tilde{A}(r_1)$, $\tilde{a}_1(r_1)$ and $\tilde{b}(r_1)$ for different r_1, and the results are summarized in table 3. From the results listed in table 3, we notice that we have $\tilde{A}(\frac{1}{3}) = \pi/8$, $\tilde{A}(1) = \pi/4$, and $\tilde{A}(3) = \pi/2$, as indicated in figure 2(*a*). Note that the behaviour of $\tilde{A}(r_1)$ as a function of r_1 is given in figure 2(*b*) by the curve $r_2 = 0$.

In conclusion, we performed a detailed study on coupling-anisotropy and finite-size effects in interfacial tension of the Ising model on a rectangular lattice and infinitely long cylinder,

Table 3. The values of the parameters in the scaling function, $\tilde{\Sigma}(z; r_1) = \tilde{a}_{L_y}(r_1) + \tilde{b}(r_1)z$, with $\tilde{a}_{L_y}(r_1) = \tilde{A}(r_1)[1 + \tilde{a}_1(r_1)y + \cdots]$ and $y = 1/L_y^2$, for an Ising cylinder with a different coupling ratio, r_1.

r_1	$\tilde{A}(r_1)$	$\tilde{a}_1(r_1)$	$\tilde{b}(r_1)$
8	3.0213(1)	3.259(5)	−1.510(4)
7	2.7565(5)	2.747(9)	−1.470(1)
6	2.4823(2)	2.281(5)	−1.429(8)
5	2.1962(2)	1.831(3)	−1.361(6)
4	1.8944(9)	1.416(8)	−1.278(9)
3	1.5707(9)	1.043(3)	−1.202(1)
2	1.2124(0)	0.692(0)	−1.081(3)
1	0.7853(9)	0.411(3)	−0.879(0)
$\frac{1}{2}$	0.5087(8)	0.292(4)	−0.696(6)
$\frac{1}{3}$	0.3927(0)	0.257(5)	−0.599(2)
$\frac{1}{4}$	0.3256(0)	0.241(5)	−0.533(8)
$\frac{1}{5}$	0.2808(7)	0.232(5)	−0.485(3)
$\frac{1}{6}$	0.2484(9)	0.227(3)	−0.447(7)
$\frac{1}{7}$	0.2237(7)	0.223(3)	−0.418(0)
$\frac{1}{8}$	0.2041(7)	0.220(0)	−0.393(3)

based on the analytic solutions of the partition functions. We summarize and discuss our results as follows:

(i) With the proposed form of the scaling function of equation (3) or (8), our data strongly indicated that the leading order of the finite-size effect in $a_{L_x}(r_1, r_2)$ or $\tilde{a}_{L_y}(r_1)$ is of the order $1/L^2$. This reflects the fact that the finite-size correction is very small.

(ii) The amplitude of the interfacial tension at the critical point, $A(r_1, r_2)$ decreases with the coupling ratio and increases with the aspect ratio. For an Ising cylinder, we have $\tilde{A}(r_1) = \pi/8$, $\pi/4$, and $\pi/2$ for the coupling ratio $\frac{1}{3}$, 1 and 3.

(iii) The value of the parameter $\tilde{b}(r_1)$ for any coupling ratio r_1 is always less than zero. This is due to the fact shown in figure 1 that σ decreases when the temperature decreases from the critical point.

(iv) For the Ising model on a rectangular lattice, we can use equations (2) and (3) to write the interfacial tension as

$$\sigma(t, r_1; L_x, L_y) = b(r_1, r_2)t\left[1 + \frac{1}{L_x t}\frac{a_{L_x}(r_1, r_2)}{b(r_1, r_2)}\right]. \tag{45}$$

When we compare this equation with the form of the scaling function

$$F(x) = 1 + \frac{B}{x} \tag{46}$$

with $x = L_x t$, used by Mon and Jasnow [3], we have

$$B = \frac{a_{L_x}(r_1, r_2)}{b(r_1, r_2)} = \frac{A(r_1, r_2)}{b(r_1, r_2)}\left[1 + \frac{a_1(r_1, r_2)}{L_x^2} + \cdots\right] \tag{47}$$

and if the finite-size correction is neglected, we have $B = 0.9785$ for $r_1 = 1$ and $r_2 = 1$. Similar results also hold for Ising cylinders, and we have $B = -0.8935$ for $r_1 = 1$.

Acknowledgments

The authors wish to thank V N Plechko for useful discussions. This work was partially supported by the National Science Council of Republic of China (Taiwan) under the Grant No NSC 88-2112-M-033-002

References

[1] Park H and den Nijs M 1988 *Phys. Rev.* B **38** 565
[2] Privman V and Fisher M E 1983 *J. Stat. Phys.* **33** 385
[3] Mon K K and Jasnow D 1984 *Phys. Rev.* A **30** 670
[4] Onsager L 1944 *Phys. Rev.* **65** 117
[5] Kaufman B 1949 *Phys. Rev.* **76** 1232
[6] Kac M and Ward J C 1952 *Phys. Rev.* **88** 1332
[7] Green H S and Hurst C A 1964 *Order–Disorder Phenomena* (New York: Interscience)
[8] Shultz T D, Mattis D C and Lieb E H 1964 *Rev. Mod. Phys.* **36** 856
[9] Plechko V N 1985 *Theor. Math. Phys.* **64** 748
[10] Plechko V N 1988 *Physica* A **152** 51
[11] Plechko V N 1998 *Phys. Lett.* A **239** 289
[12] Morita T 1992 *J. Phys. Soc. Japan* **61** 2694
[13] Lipowski A and Suzuki M 1992 *J. Phys. Soc. Japan* **61** 4356
[14] Angelini L, Caroppo D, Pellicoro M and Villani M 1992 *J. Phys. A: Math. Gen.* **25** 5423